

Supplemental Figures

Chemotherapy weakly contributes to predicted neoantigen expression in
ovarian cancer

*Timothy O'Donnell, Elizabeth L. Christie, Arun Ahuja, Jacqueline Buros, B. Arman
Aksoy, David D. L. Bowtell, Alexandra Snyder, Jeff Hammerbacher*

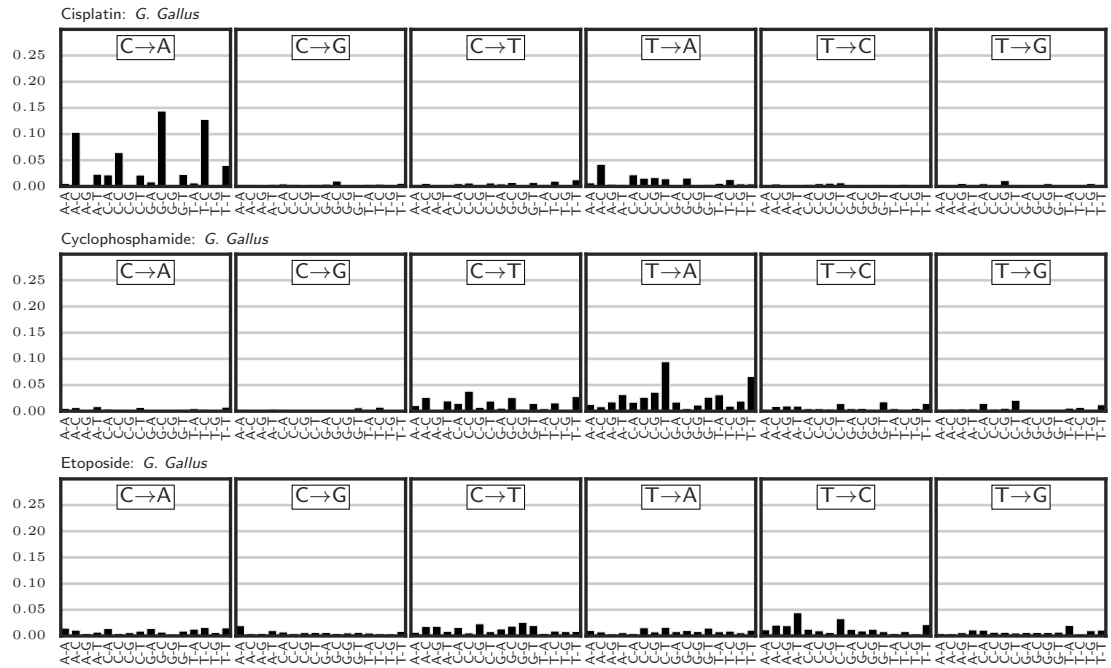


Figure S1: Mutational signatures extracted from Szikriszt et al. [1]

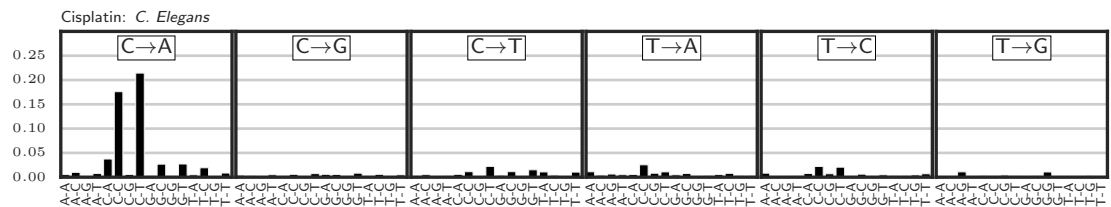


Figure S2: Mutational signature extracted from Meier et al. [2]

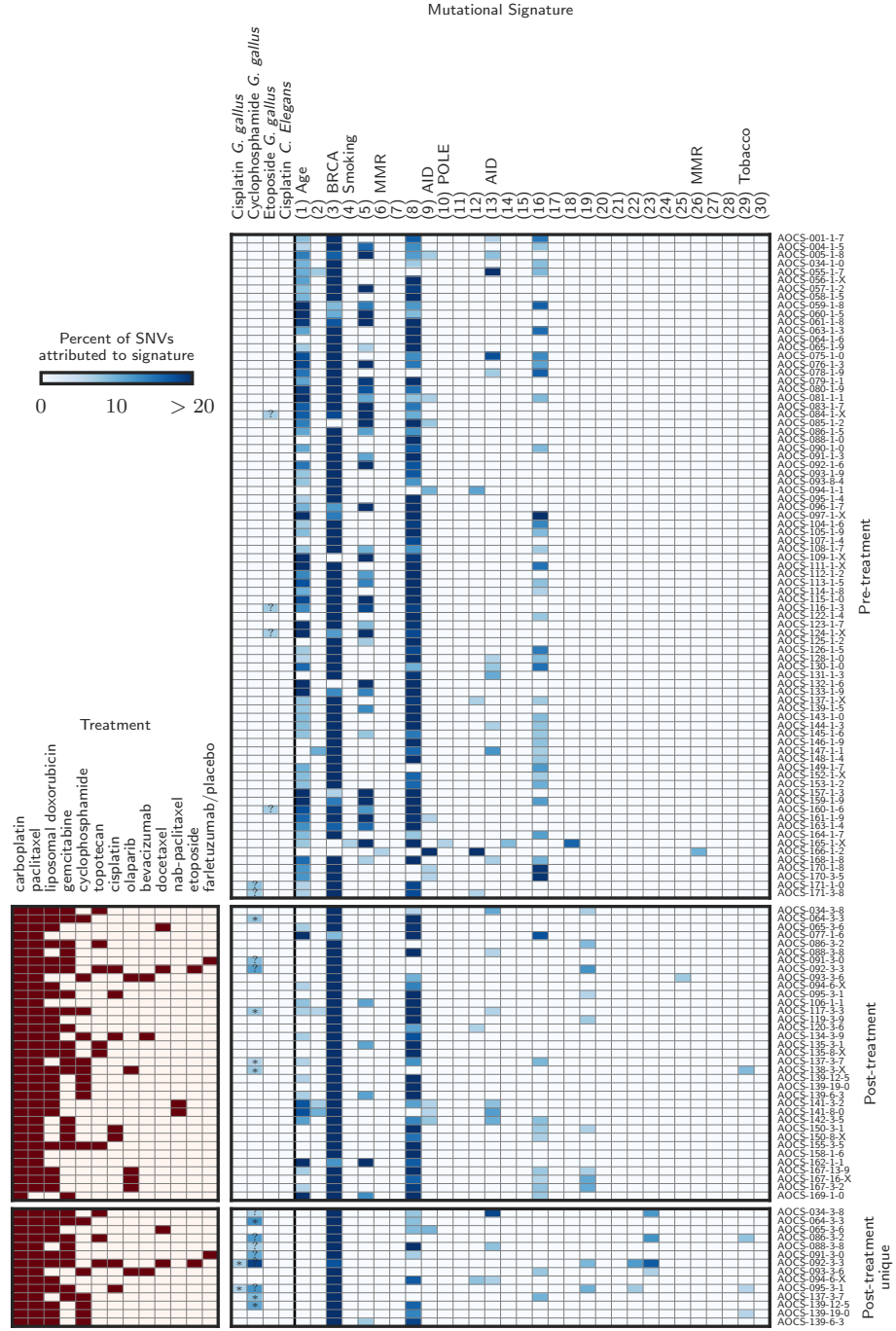


Figure S3: **Detected mutational signatures across all samples.** The symbols are as in main text Figure 1. The top and middle panels show the signature deconvolutions for all pre- and post-treatment samples, respectively. The bottom panel shows deconvolutions for the mutations unique to the paired post-treatment samples, requiring high coverage and no variant reads in the donor-matched pre-treatment sample.

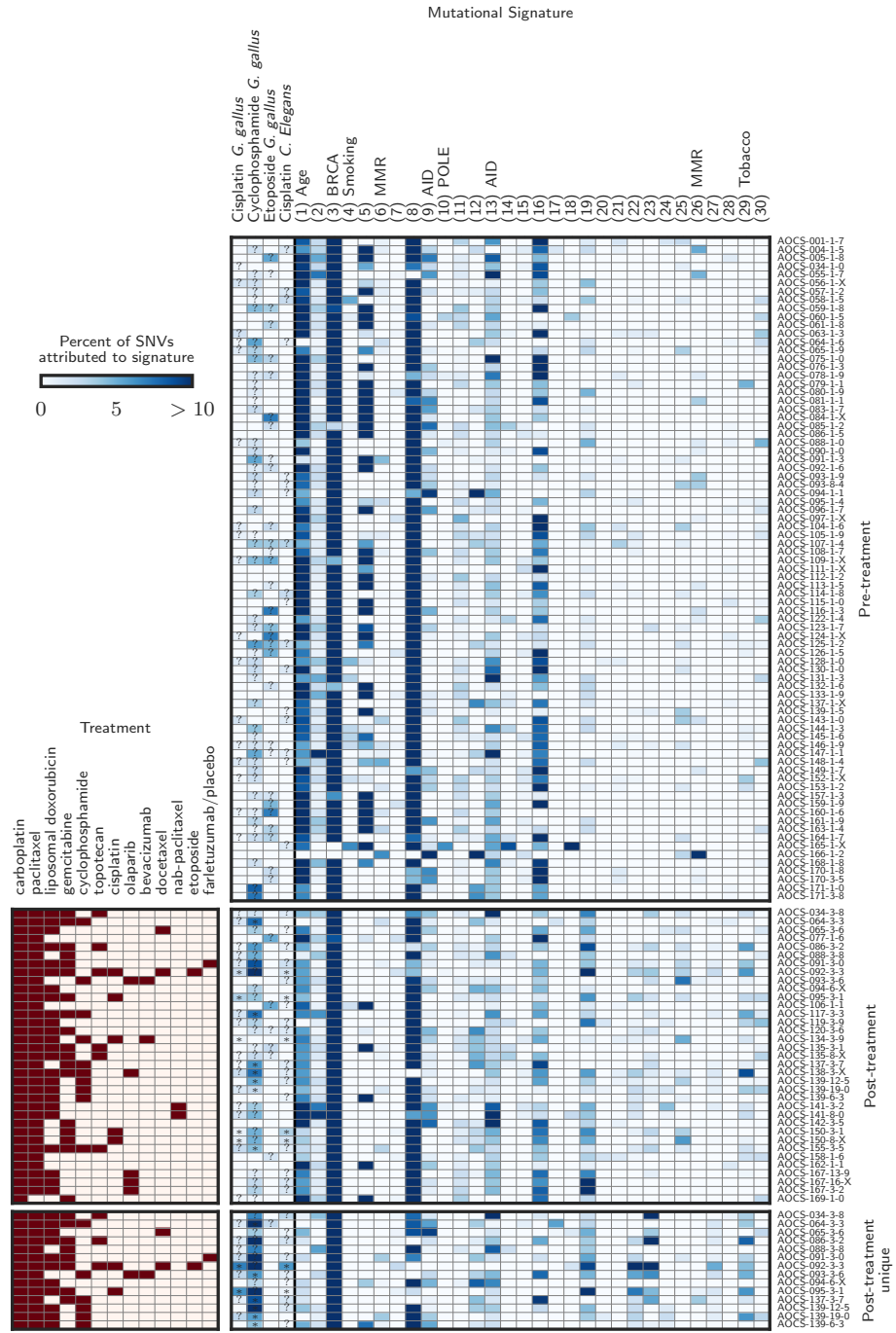


Figure S4: **Mutational signature deconvolutions without any threshold of detection.** Here, signatures accounting for less than the 6% recommended detection threshold are included.

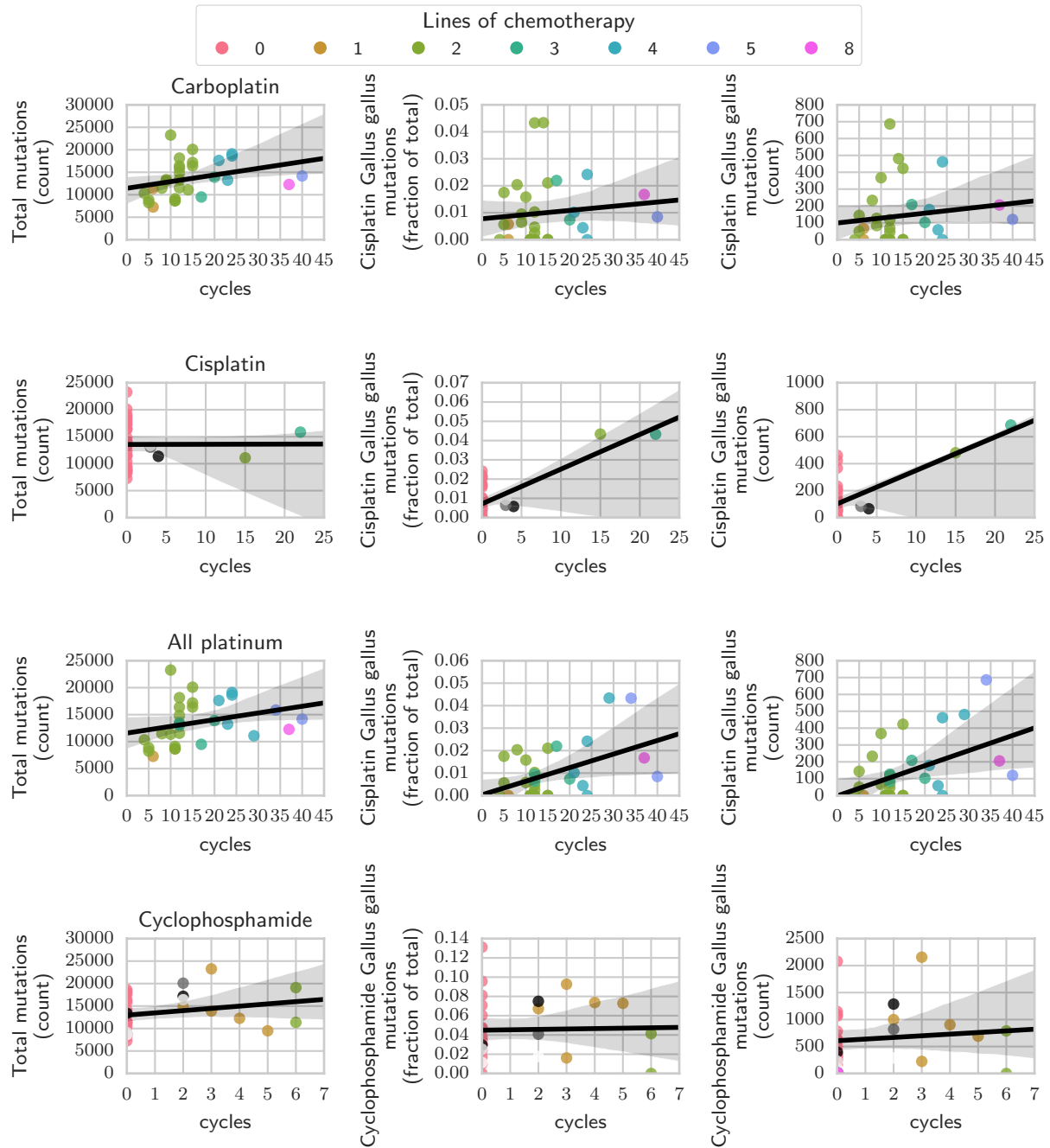


Figure S5: Association of chemotherapy cycles on total genome-wide mutation burden (left) and mutations attributed to the *G. Gallus* cisplatin and cyclophosphamide signatures as a fraction of total (middle) and as a count (right). The total mutation burden includes both SNVs and indels. Cycles indicated are of the labelled chemotherapy. Colors indicate the number of lines of chemotherapy.

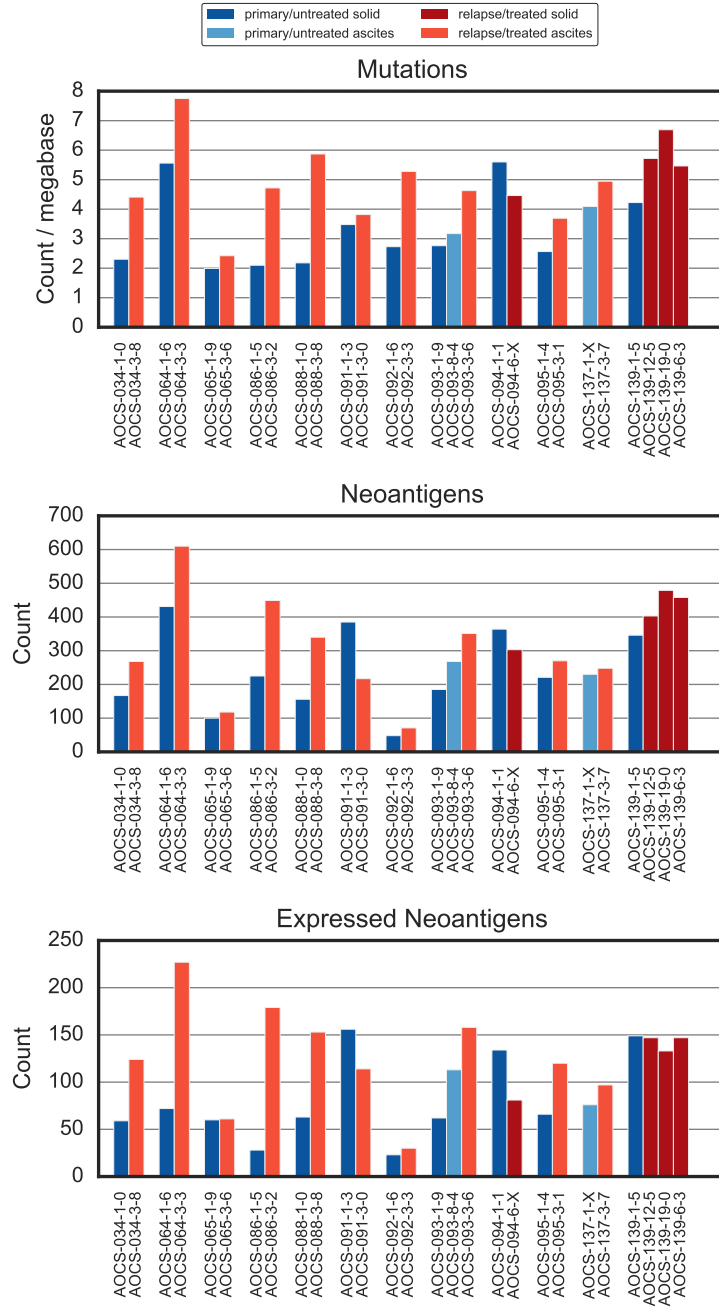


Figure S6: Mutations, neoantigens, and expressed neoantigens for donor-matched primary/untreated and relapse/treated samples.

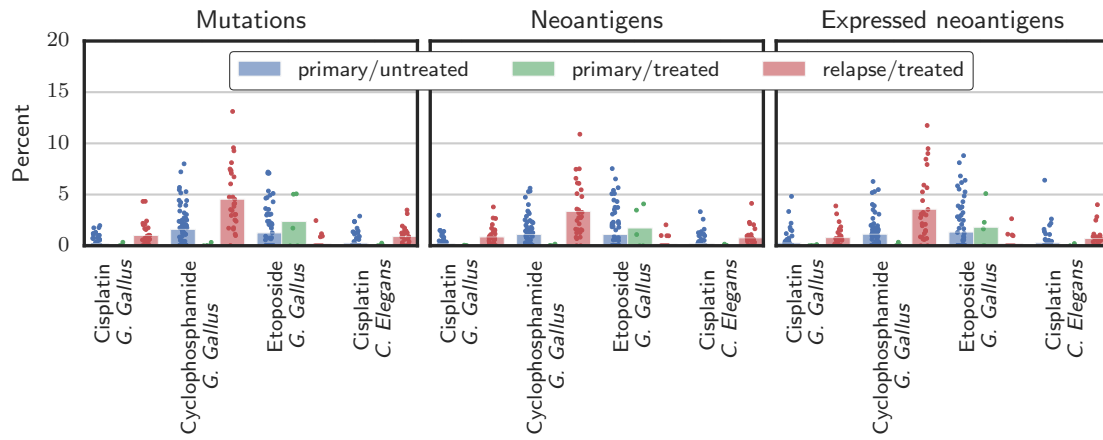


Figure S7: **Contribution of chemotherapy SNV signatures.** The fraction of each sample's mutations, neoantigens, and expressed neoantigens attributed to putative chemotherapy signatures is shown. Bars give the mean, and points indicate individual samples.

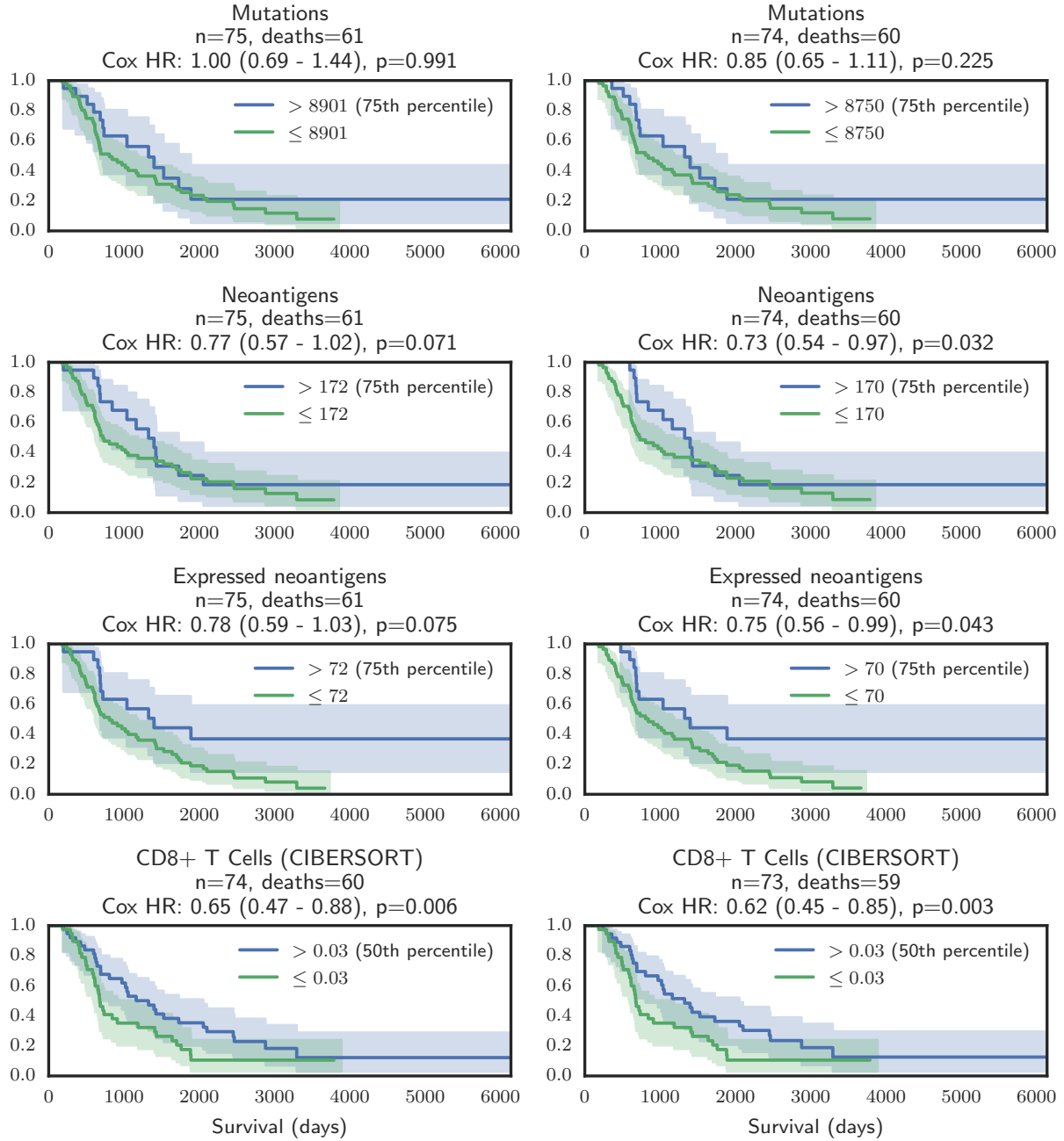


Figure S8: **Kaplan-Meier curves for patients split by the number of mutations, neoantigens, expressed neoantigens, or estimate of CD8+ T cell infiltrate.** Only primary/untreated solid-tissue samples are considered. The survival curves split the samples into high and low groups using a percentile threshold, but the annotated Cox hazard ratio (HR) and p-value correspond to a regression model that treats the value of interest as a continuous covariate. The left plots include all primary/untreated samples; the right plots exclude outlier sample AOCs-166-1-2. The CD8+ T cell analyses exclude sample AOCs-056-1-X, which failed deconvolution.



Figure S9: RNA-seq based immune deconvolution (CIBERSORT) of solid-tissue samples.

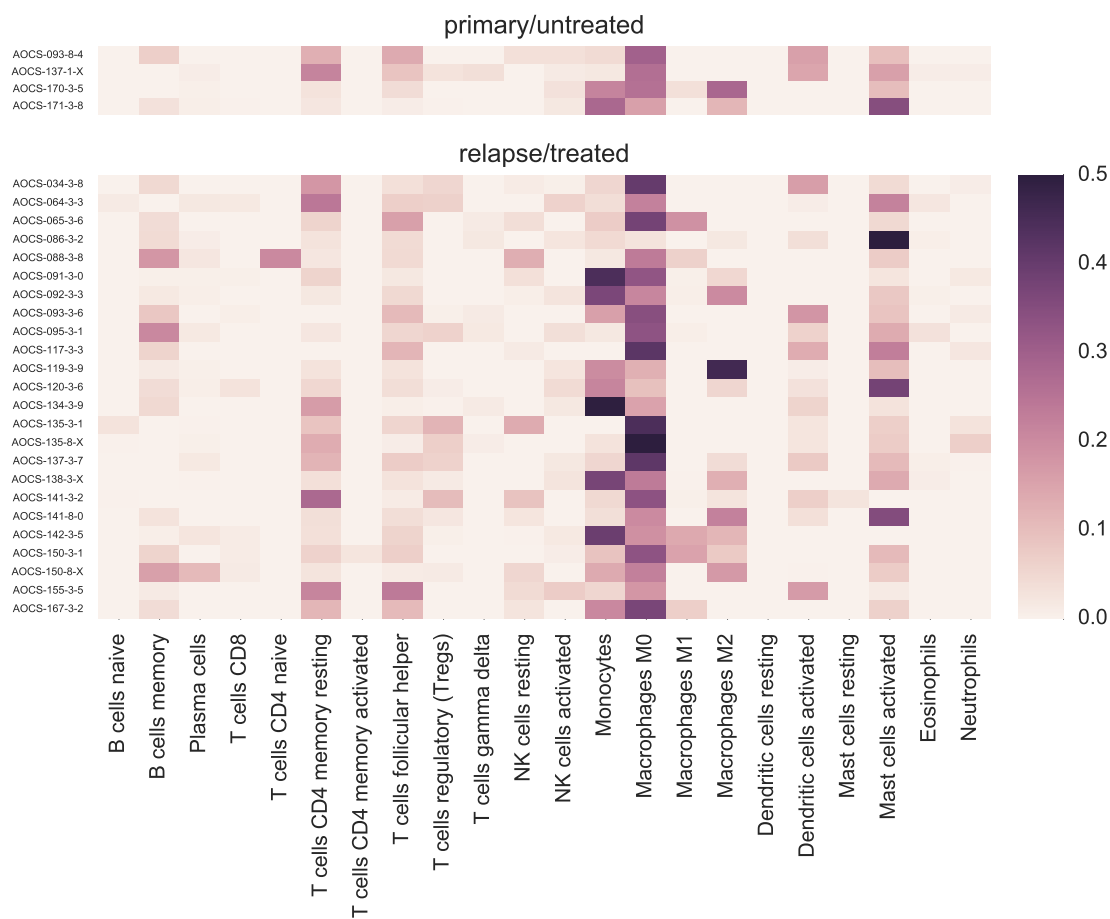


Figure S10: RNA-seq based immune deconvolution (CIBERSORT) of ascites samples.

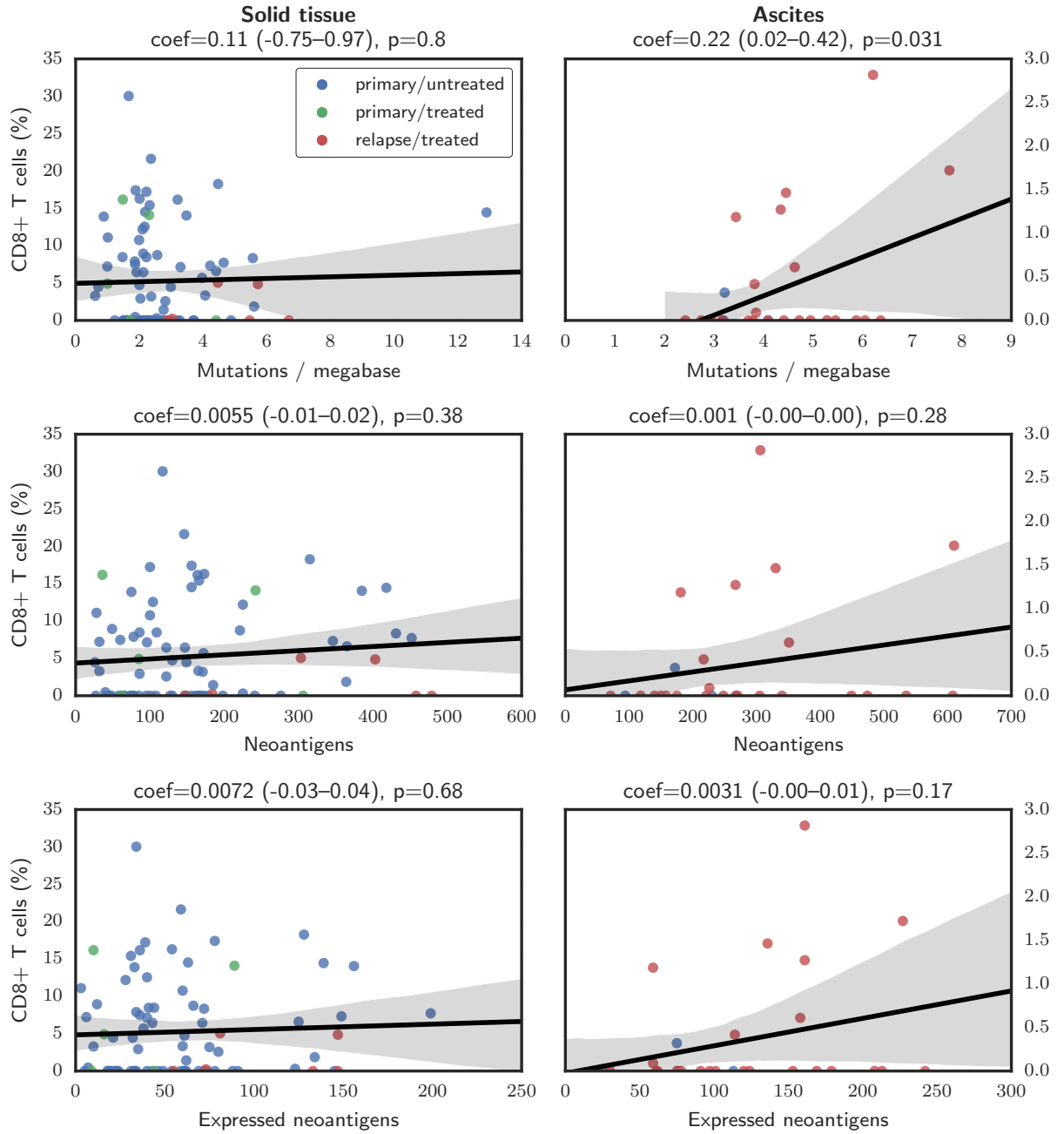


Figure S11: Relationship between CD8+ T cell infiltrate estimated by CIBERSORT and mutations, neoantigens, or expressed neoantigens for solid tissue (left) and ascites (right) samples. Colors indicate sample time point.

References

- [1] B. Szikriszt, Á. Póti, O. Pipek, M. Krzystanek, N. Kanu, J. Molnár, D. Ribli, Z. Szeltner, G. E. Tusnádý, I. Csabai, Z. Szallasi, C. Swanton, and D. Szts, “A comprehensive survey of the mutagenic impact of common cancer cytotoxics,” *Genome Biol*, vol. 17, may 2016.
- [2] B. Meier, S. L. Cooke, J. Weiss, A. P. Bailly, L. B. Alexandrov, J. Marshall, K. Raine, M. Maddison, E. Anderson, M. R. Stratton, A. Gartner, and P. J. Campbell, “C. elegans whole-genome sequencing reveals mutational signatures related to carcinogens and DNA repair deficiency,” *Genome Research*, vol. 24, pp. 1624–1636, jul 2014.